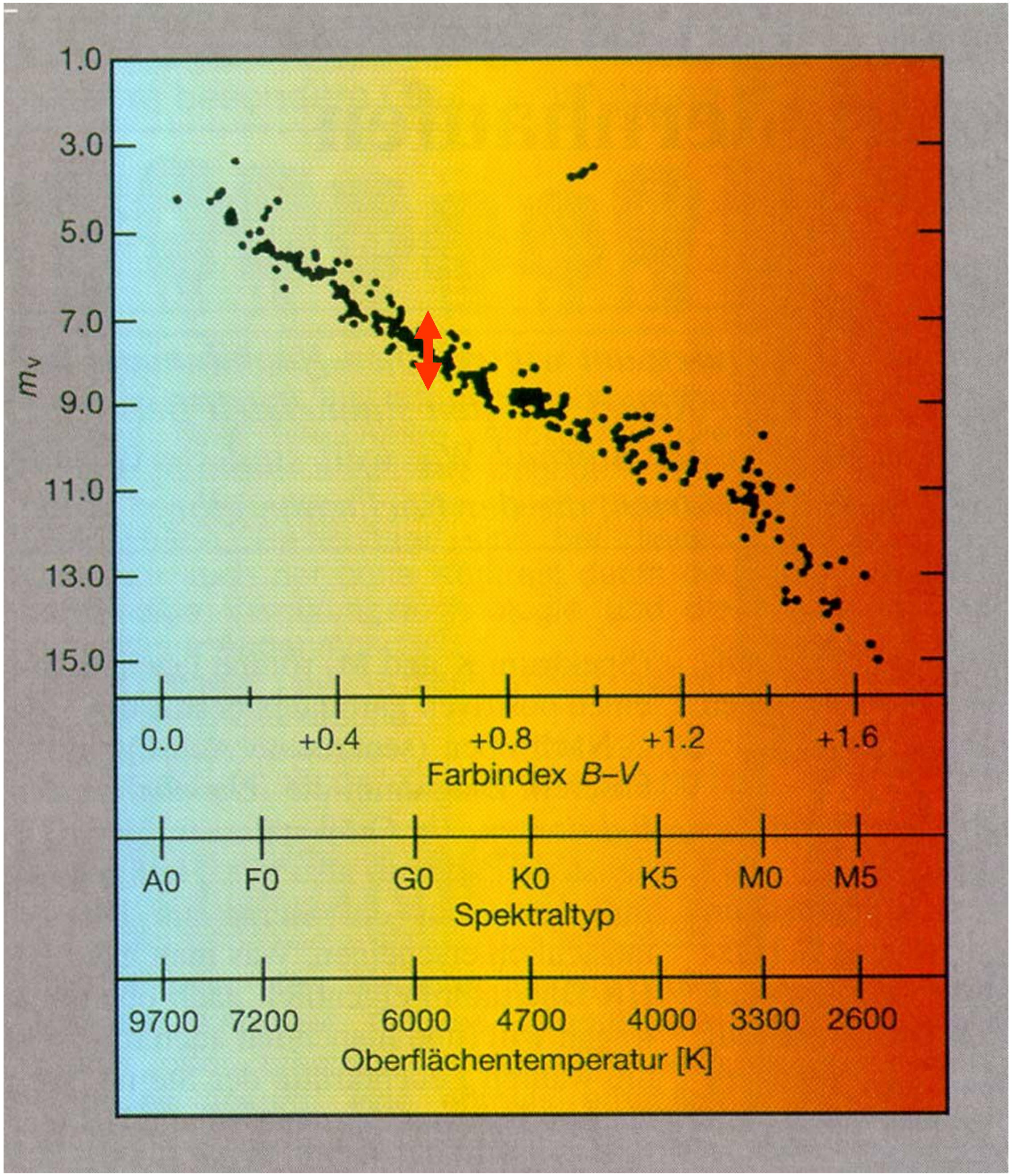

Hyades

log t = 8.90
d = 45 pc
[Fe/H] = +0.17 dex

↕ Width of Main Sequence about 1.8 mag in M_V

NO
Observational error

What are the reasons?

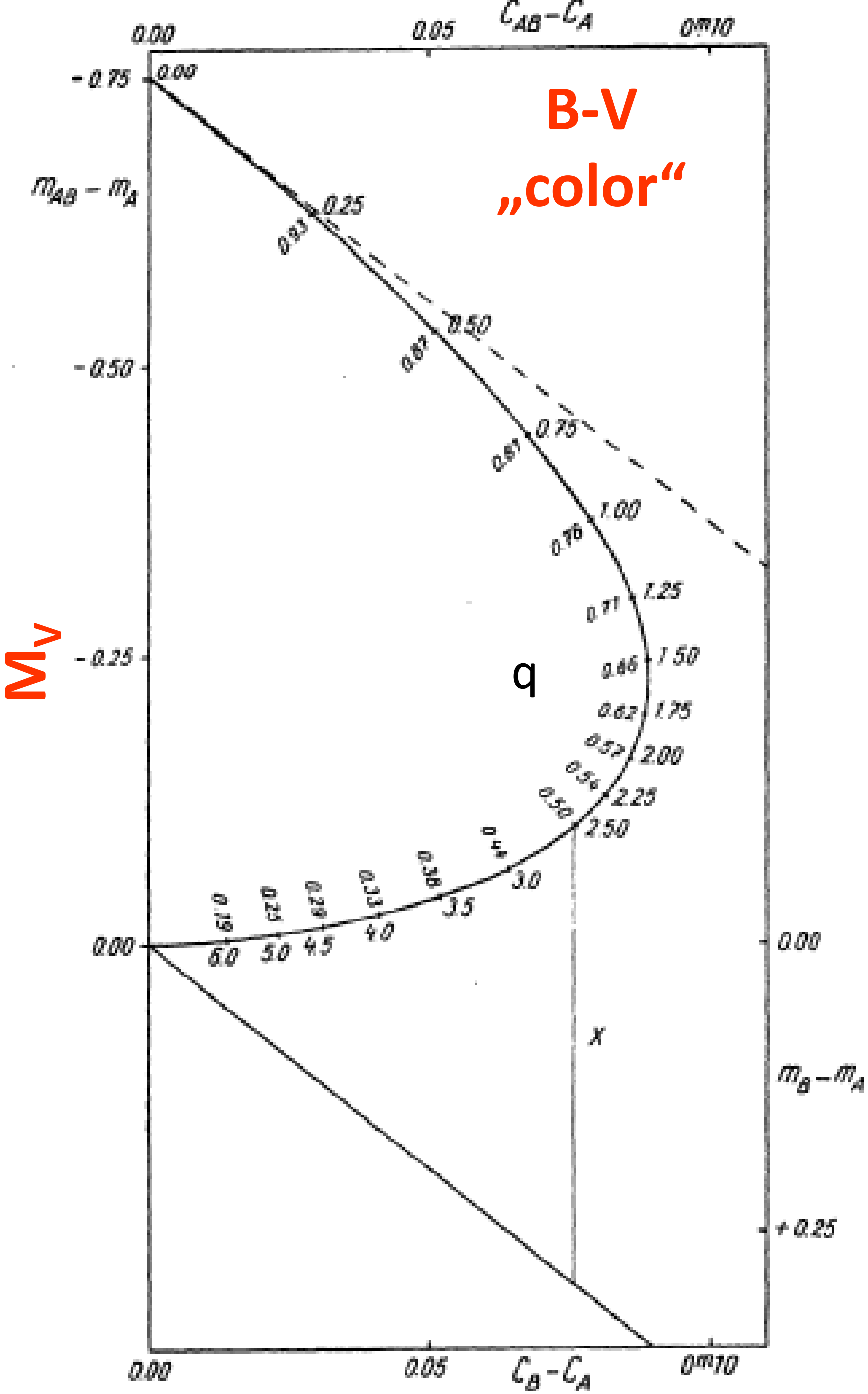

Vertical distance from the main sequence

$$x = a(C_{AB} - C_A) + V_A - V_{AB}$$

Absolute magnitude:

$$M_V = -2.5 \log (L_1 + L_2)$$

Maximum at $L_1 = L_2$ =>

$$M_V = -0.753 \text{ mag}$$

The maximal width of the main sequence due to binary systems is 0.753 mag

Haffner & Heckmann, 1937, VeGeo, 55, 77

Praesepe: Fossati et al., 2008, A&A, 483, 891

At.N.	Element	"Normal" A–type stars HD 72846	HD 73345	HD 73450	HD 73574	HD 74028	HD 74050	HD 74587	HD 74718	Solar Abundances
3	Li	< −8.08(−; 1)	< −8.33(−; 1)	< −8.70(−; 1)	< −8.38(−; 1)			< −8.41(−; 1)	< −8.26(−; 1)	−10.99
6	C	−3.58(−; 1)	−3.44(12; 3)	−3.27(−; 1)	−3.36(18; 2)	−3.39(08; 2)	−3.52(−; 1)	−3.49(01; 2)	−3.51(04; 2)	−3.65
8	O	−3.18(−; 1)	−3.22(01; 2)				−3.70(−; 1)	−3.30(−; 1)		−3.38
11	Na	−5.44(01; 2)	−5.37(01; 2)	−6.28(−; 1)	−5.57(02; 2)	−5.98(−; 1)	−5.64(13; 2)	−5.61(02; 2)	−5.70(14; 2)	−5.87
12	Mg	−4.18(08; 3)	−4.18(02; 3)	−5.02(18; 2)	−4.37(04; 3)	−4.86(08; 3)	−4.22(05; 4)	−4.56(08; 3)	−4.52(01; 2)	−4.51
14	Si	−4.62(16; 2)	−4.67(−; 1)	−4.13(−; 1)	−4.19(−; 1)	−4.17(−; 1)	−4.37(−; 1)	−4.16(−; 1)	−4.25(−; 1)	−4.53
16	S	−4.71(04; 2)	−4.44(03; 4)	−4.35(−; 1)	−4.61(02; 2)	−4.26(01; 2)		−4.50(04; 2)	−4.28(11; 2)	−4.90
20	Ca	−5.17(−; 1)	−5.39(09; 6)	−5.95(06; 4)	−5.86(16; 5)	−5.37(16; 2)	−6.13(06; 2)	−5.49(15; 6)	−5.68(02; 3)	−5.73
21	Sc	−8.88(−; 1)	−8.63(07; 3)	−8.57(14; 3)	−8.89(02; 3)	−8.35(−; 1)	−8.96(27; 3)	−8.56(−; 1)	−8.69(14; 2)	−8.99
22	Ti	−6.88(03; 5)	−6.95(06; 6)	−7.30(11; 5)	−6.98(09; 5)	−6.78(−; 1)	−7.08(15; 5)	−6.83(16; 3)	−6.93(10; 5)	−7.14
24	Cr	−6.23(06; 3)	−6.22(08; 2)	−6.56(08; 3)	−6.19(16; 3)	−6.23(12; 4)	−6.48(10; 3)	−6.05(13; 4)	−6.44(20; 5)	−6.40
25	Mn		−6.37(−; 1)	−6.88(−; 1)	−6.52(02; 2)	−6.77(−; 1)	−6.61(−; 1)	−6.62(04; 2)	−6.71(−; 1)	−6.65
26	Fe	−4.55(18; 42)	−4.33(11; 61)	−4.62(09; 15)	−4.49(10; 30)	−4.50(09; 18)	−4.44(13; 16)	−4.28(10; 33)	−4.61(11; 26)	−4.59
28	Ni	−5.70(18; 2)	−5.58(11; 4)	−5.82(16; 2)	−5.62(08; 4)	−5.93(14; 3)	−5.60(15; 3)	−5.84(−; 1)	−5.68(02; 3)	−5.81
39	Y	−9.75(−; 1)	−9.46(−; 1)	−9.83(−; 1)	−9.20(−; 1)	−9.56(−; 1)	−9.26(−; 1)	−9.13(−; 1)	−9.10(−; 1)	−9.83
56	Ba	−9.48(−; 1)	−9.30(06; 2)	−9.50(02; 2)	−8.98(04; 2)	−9.65(−; 1)	−9.52(01; 2)	−8.96(25; 2)	−9.15(−; 1)	−9.87
	T_{eff}	8045	7993	7270	7662	7750	7872	7500	7600	
	$\log g$	3.50	3.96	4.20	4.00	4.50	3.66	4.20	4.00	
	υ_{mic}	2.5	2.6	2.7	2.6	2.6	2.6	2.7	2.7	
	$\upsilon \sin i$	119	85	138	102	150	188	90	155	

Fe: -4.28 to -4.62dex; 0.34 dex

Metallicity => different opacity

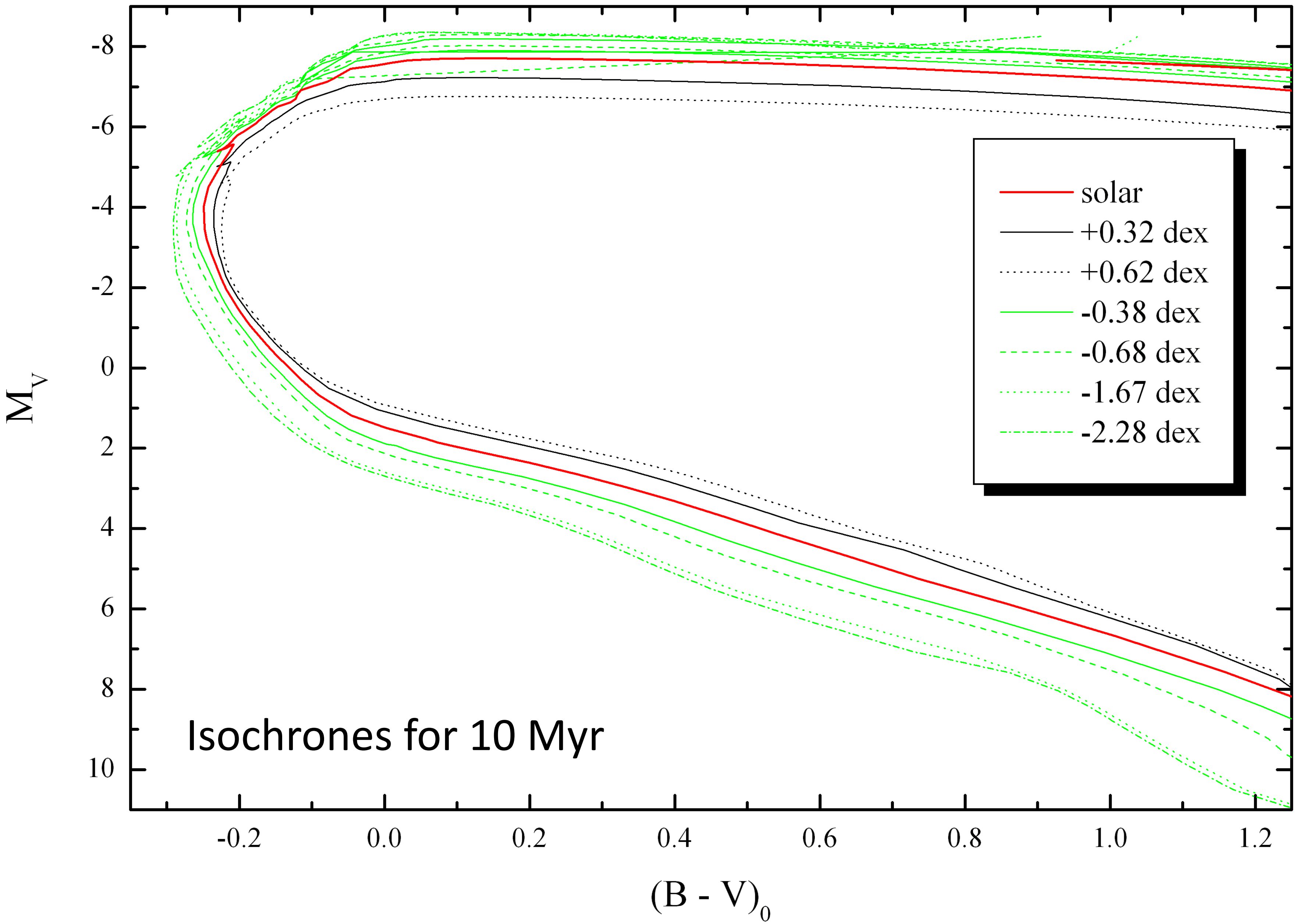

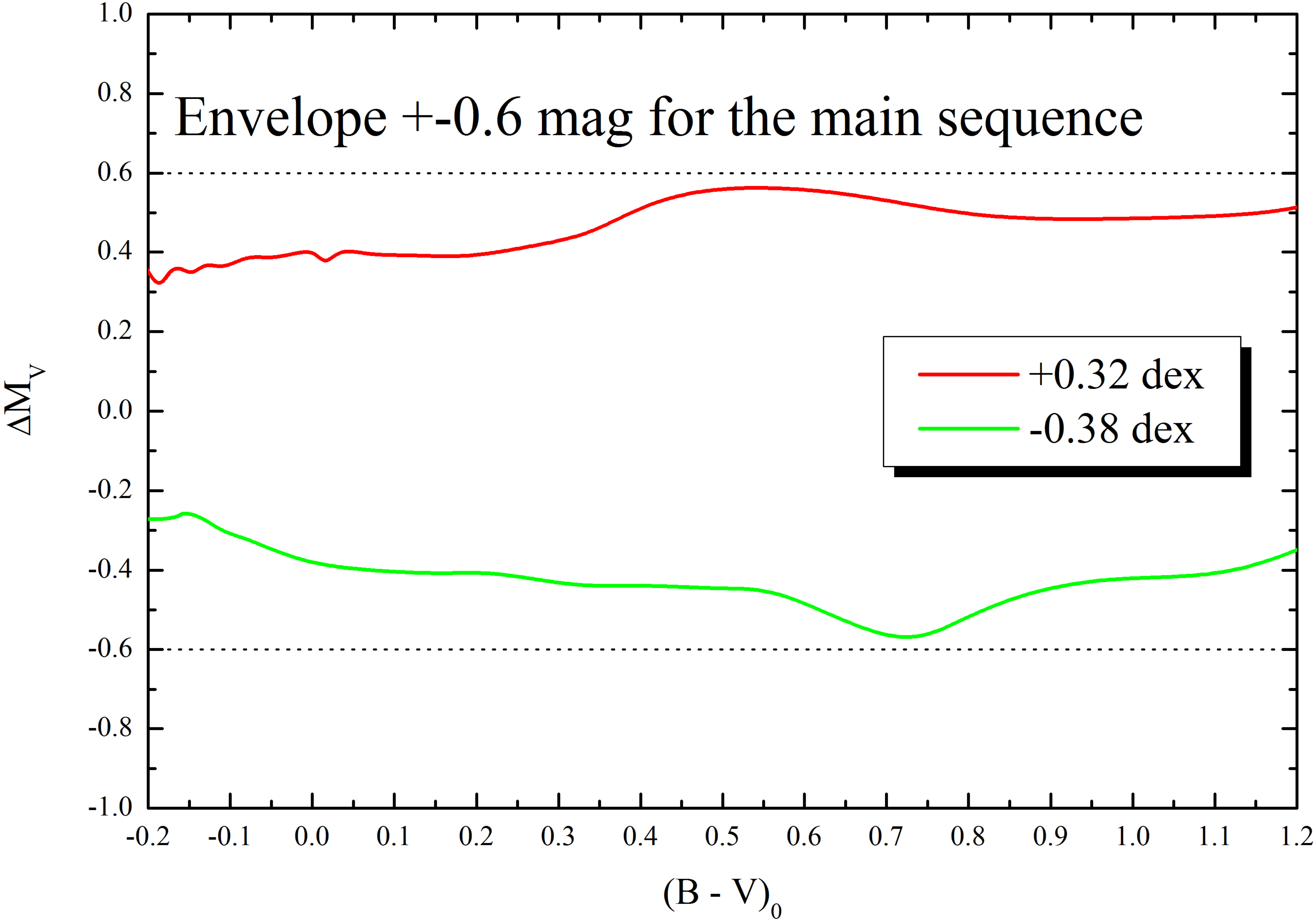

Envelope +-0.6 mag for the main sequence
+0.32 dex
-0.38 dex
ΔM_V
$(B - V)_0$
1.0
0.8
0.6
0.4
0.2
0.0
-0.2
-0.4
-0.6
-0.8
-1.0
-0.2
-0.1
0.0
0.1
0.2
0.3
0.4
0.5
0.6
0.7
0.8
0.9
1.0
1.1
1.2

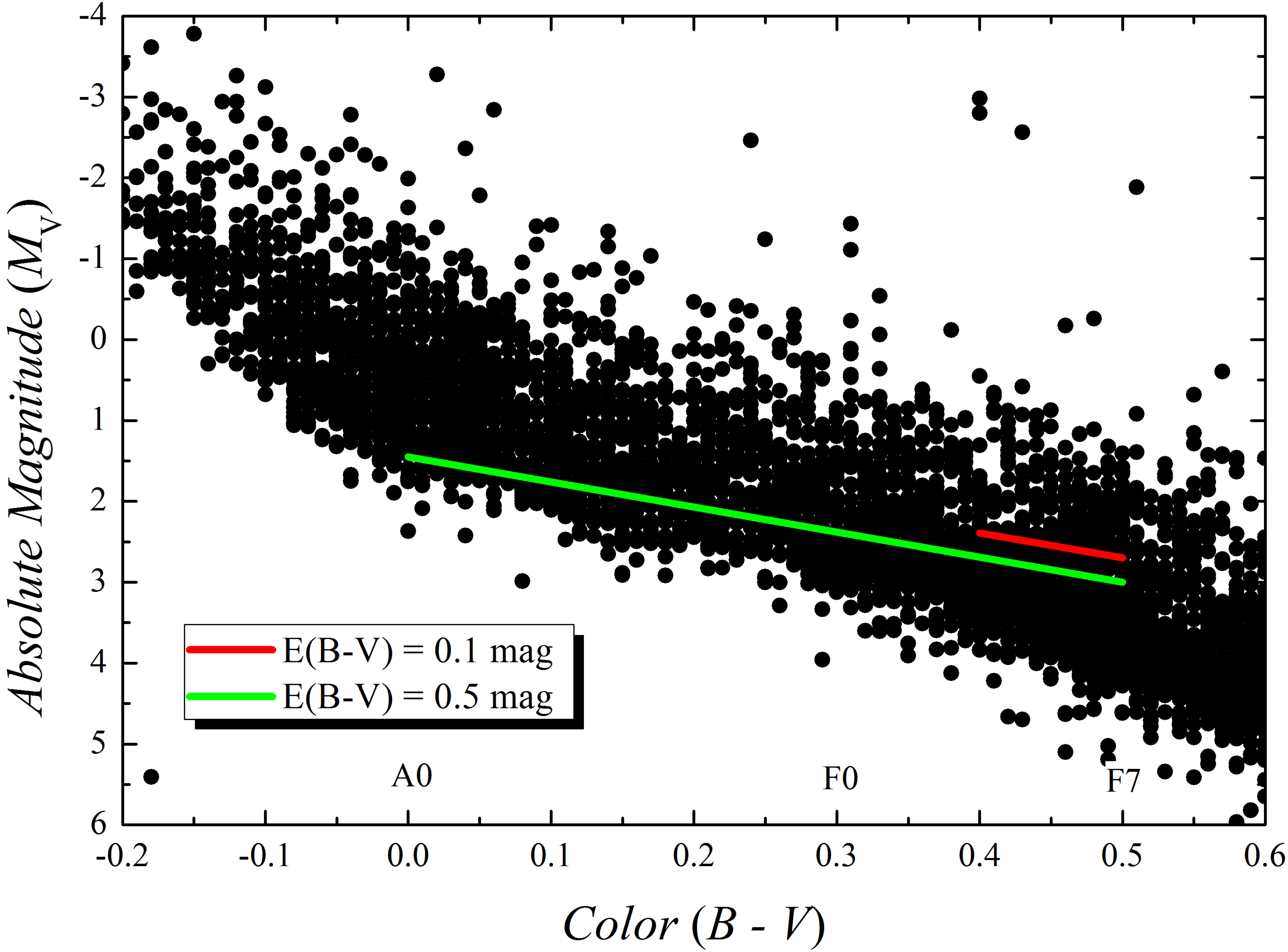

Absolute Magnitude (M_V)
Color (B - V)
E(B-V) = 0.1 mag
E(B-V) = 0.5 mag
A0
F0
F7
-4
-3
-2
-1
0
1
2
3
4
5
6
-0.2
-0.1
0.0
0.1
0.2
0.3
0.4
0.5
0.6

Slettebak et al., 1980, ApJ, 242, 171

Rotation

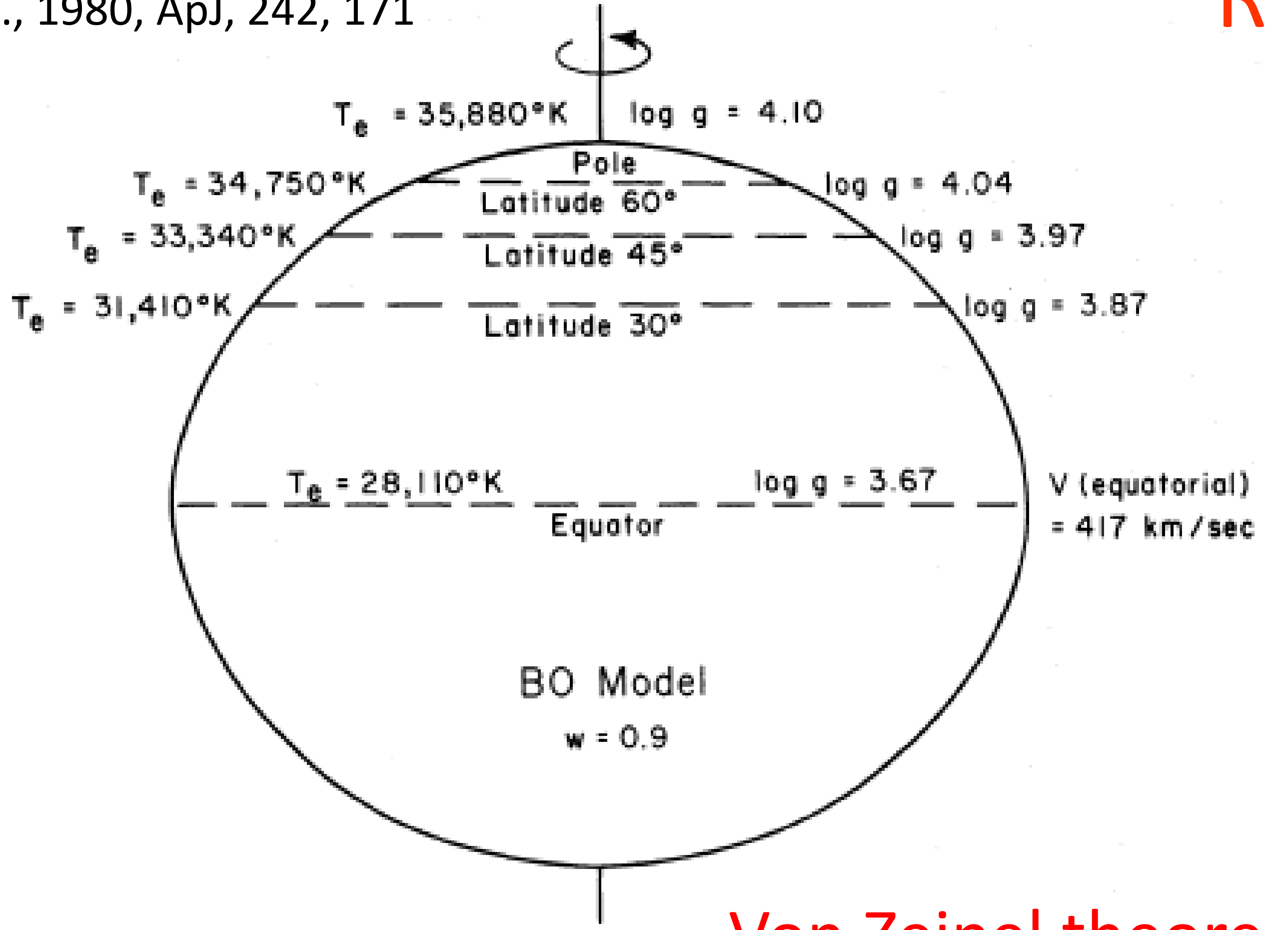

Von Zeipel theorem (1924, MNRAS, 84, 665)

Energy generation rate $\epsilon = (\text{const})\left(1 - \frac{\omega^2}{2\pi G\rho}\right)$

From the rotational velocity => ε => T_{eff} and L (log g)

Vega

Table 7
A Summary of Physical Parameters for the Pole-on Model

Parameter	Value
Equatorial radius ($R_\odot$)	2.75 ± 0.01
Polar radius ($R_\odot$)	2.40 ± 0.02
Polar effective temperature (K)	10000 ± 30
Pole-to-equator $T_{\rm eff}$ difference (K)	1410
Mean effective temperature (K)	9560 ± 30
Luminosity ($L_\odot$)	44 ± 2
Mass ($M_\odot$)	2.4 ± 0.1
Polar surface gravity (cgs, dex)	4.04 ± 0.01
Pole-to-equator log g difference (cgs, dex)	0.26
Mean surface gravity (cgs, dex)	3.95 ± 0.01
Projected rotational velocity (km s^{-1})	20.8 ± 0.2
Inclination of rotation axis (degrees)	5.7 ± 0.1
Equatorial rotational velocity (km s^{-1})	211 ± 4
Fraction of breakup velocity (km s^{-1})	0.81 ± .02

Hill et al., 2010, ApJ, 712, 250

Collins & Smith, 1985, MNRAS, 213, 519

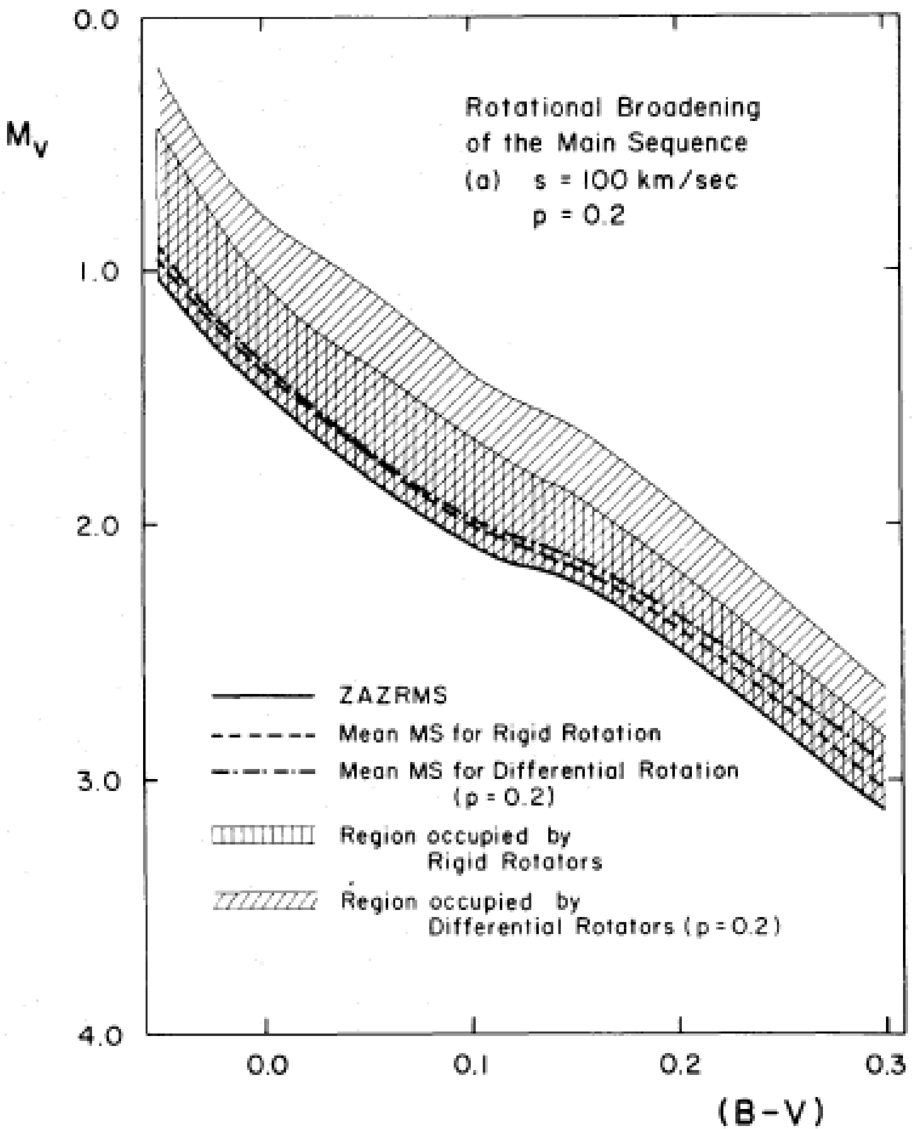

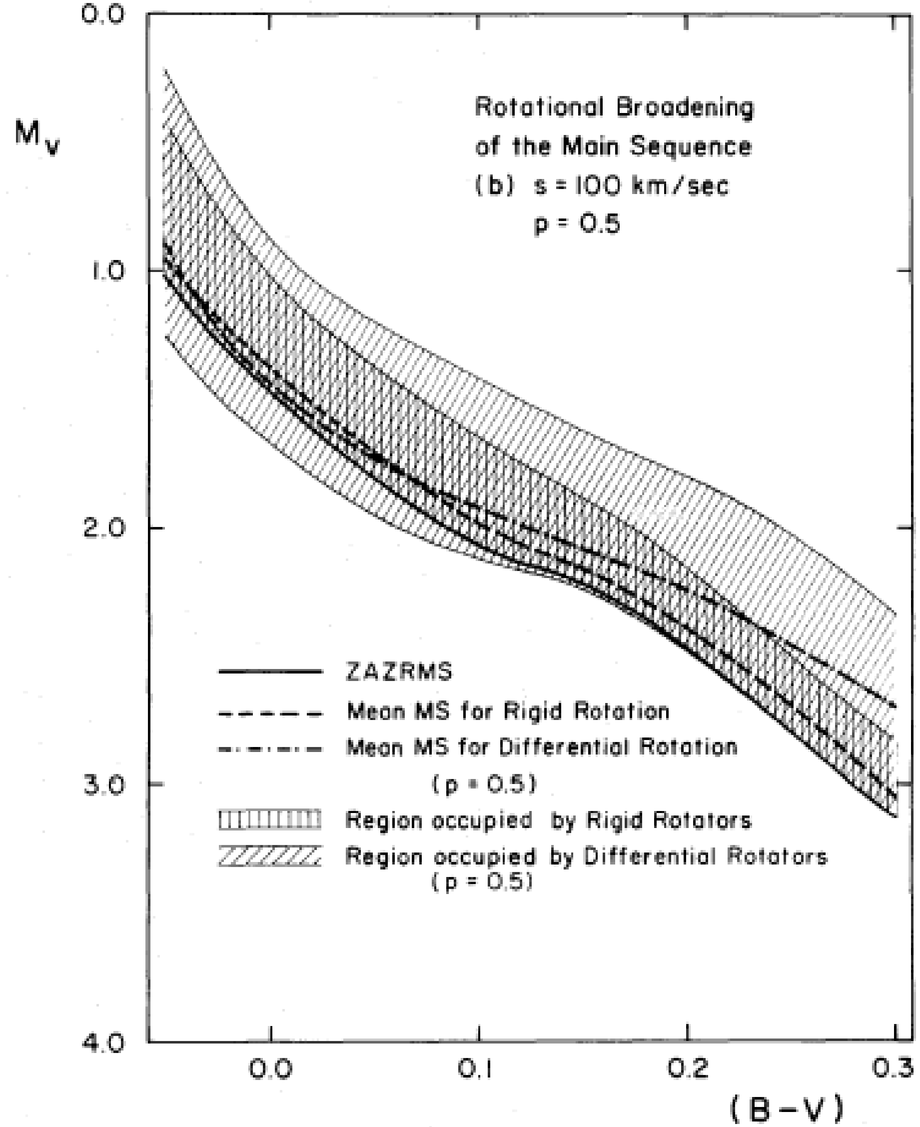

p … Degree of differential rotation

Collins & Smith, 1985, MNRAS, 213, 519

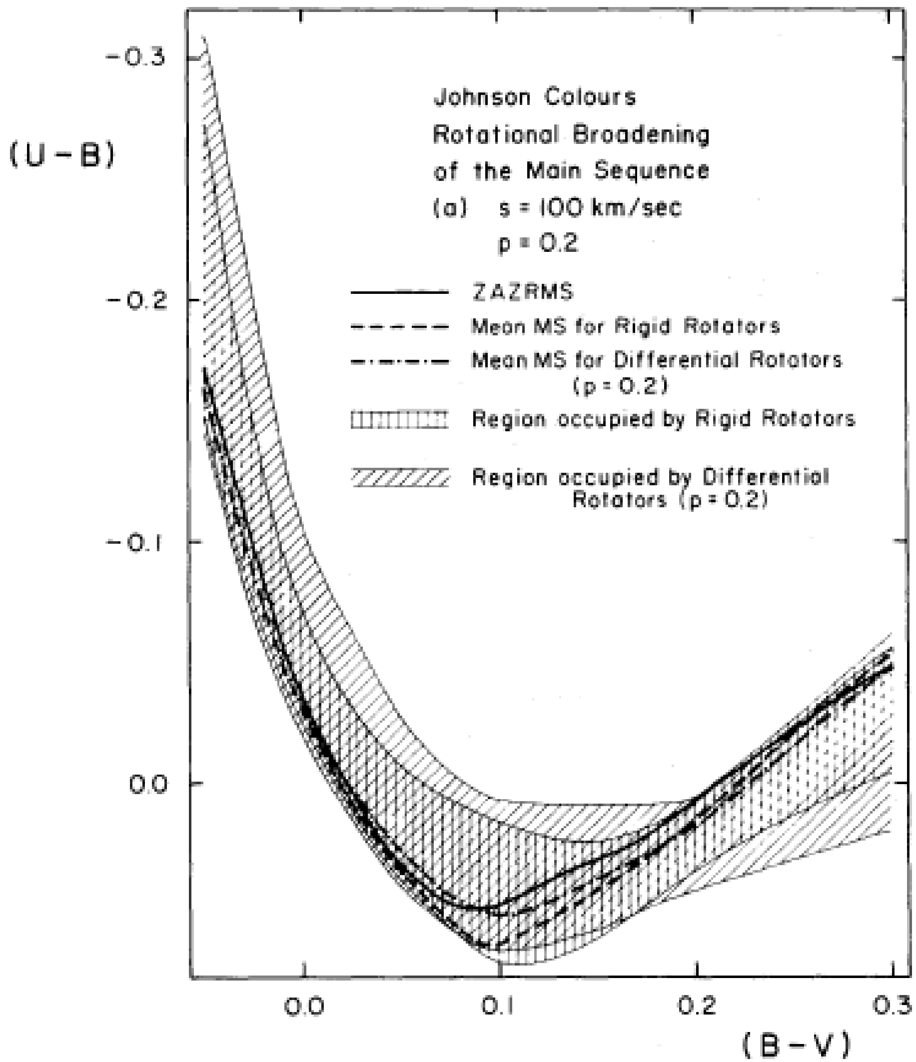

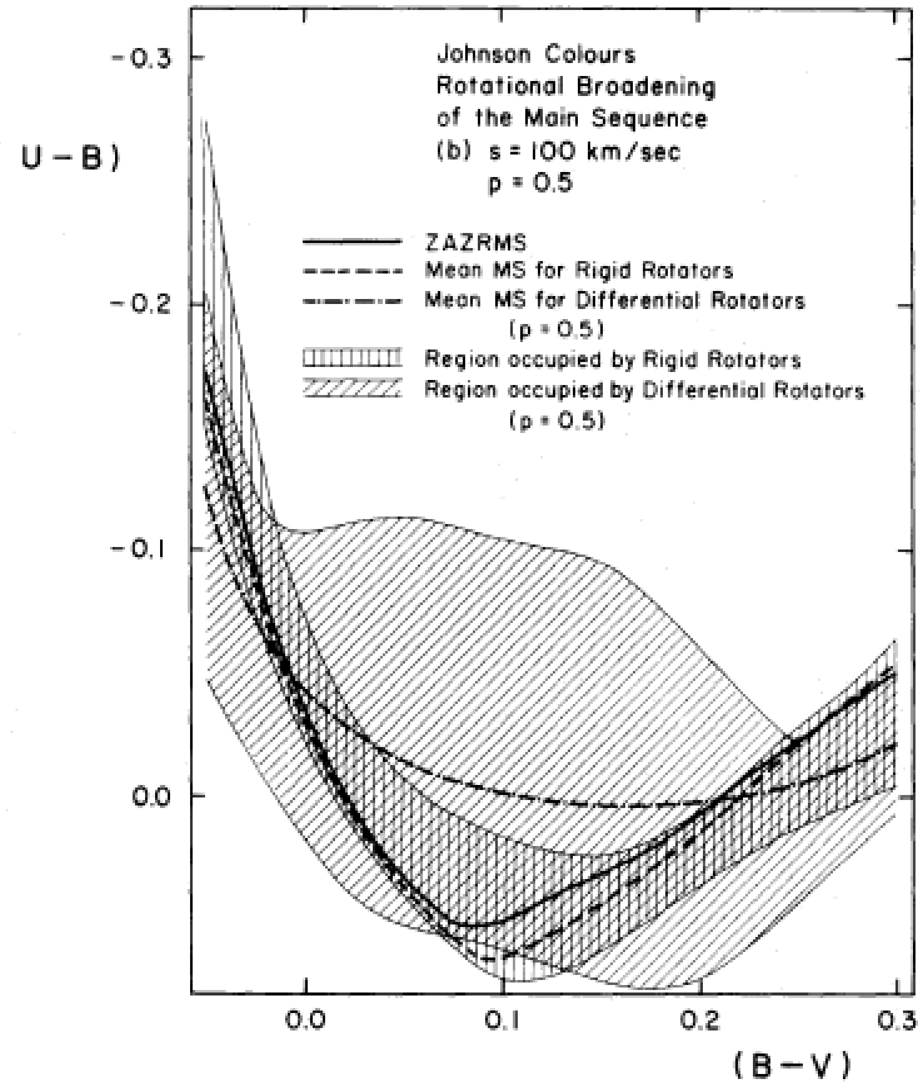

Conclusions – Width of the Main Sequence

- Differential reddening: k·ΔE(B-V)
- Spectroscopic Binaries: 0.753 mag
- Metallicity: up to 1.2 mag for M_V, but only 0.2 mag for (U – B) versus (B – V)
- Rotation: 1 mag for M_V, 0.2 (?) mag for (U – B) versus (B – V)

Binary fraction

- Important for the formation and evolution of star clusters
- Critical parameter for the IMF
- Needed for N-body numerical simulations
- Observations are biased in many respects
- Many different types of binary systems

Machida, 2008, ApJ, 682, L1

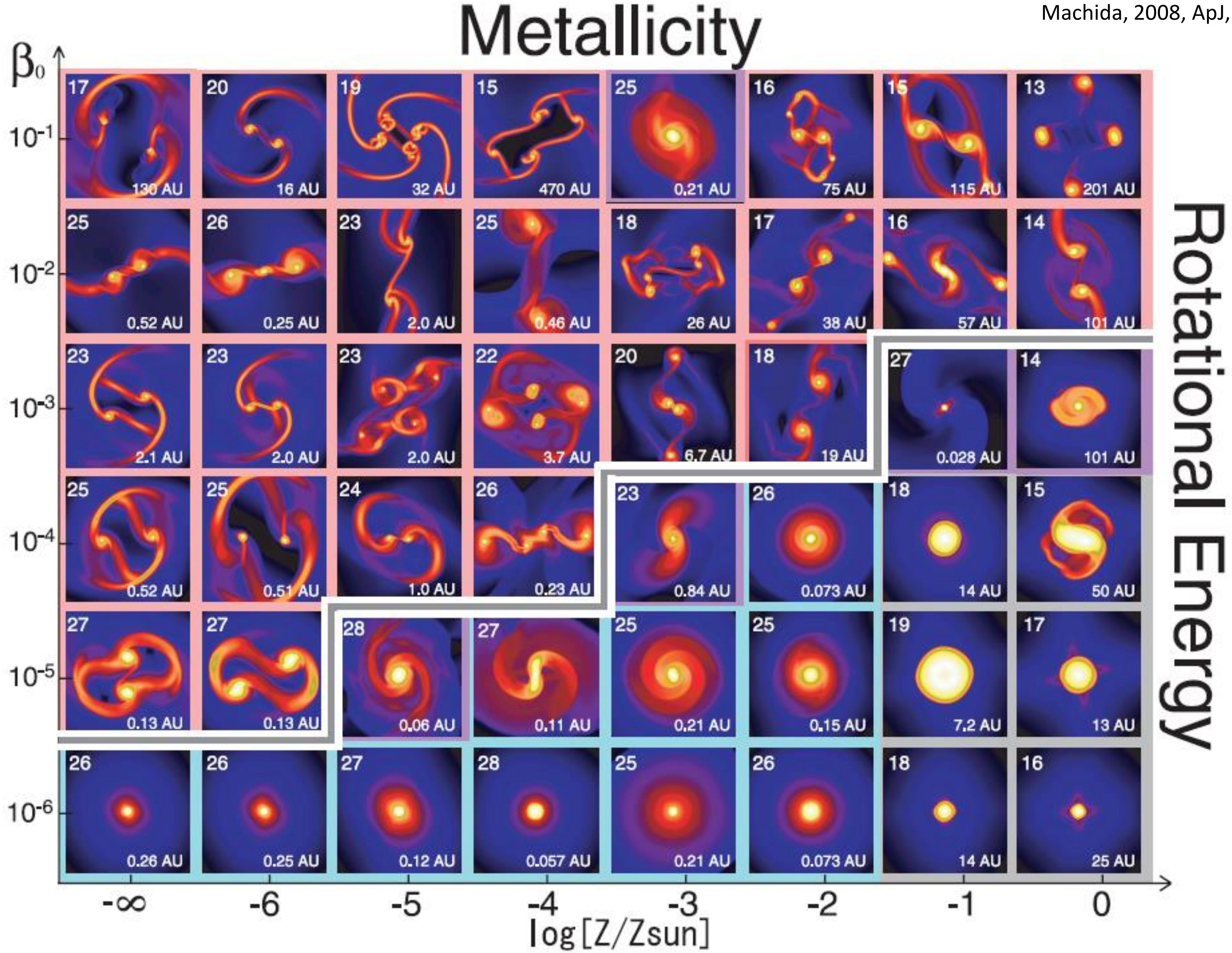

Lower metallicities seem to favour binary formation

How to observe the binary fraction?

- Photometric observations of star clusters
  1. “Cluster main sequence”
  2. Eclipsing binaries
  3. Positions (astrometric binaries)
- Spectroscopic observations
  1. Radial velocity variability
  2. Direct detection in spectrum (SB2)

Hurley & Tout, 1998, MNRAS, 300, 977

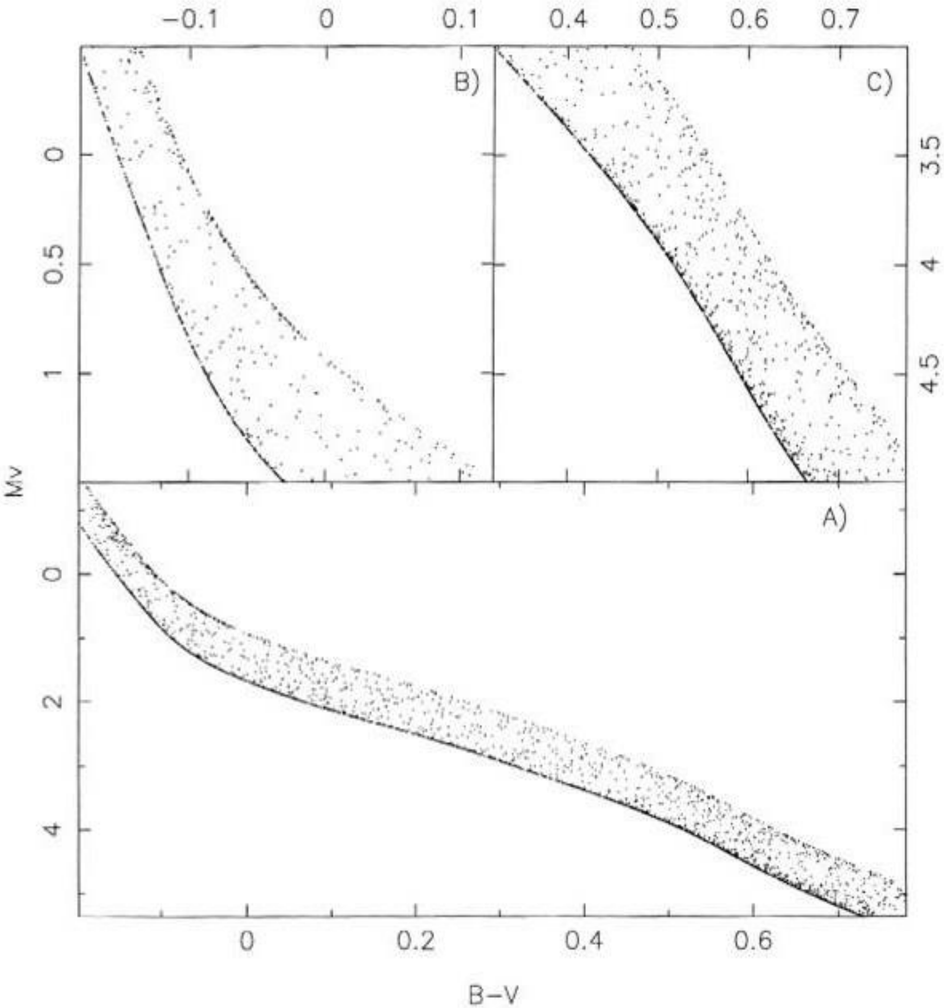

Simulation with randomly distributed mass ratios

Haffner & Heckmann, 1937, VeGeo, 55, 77

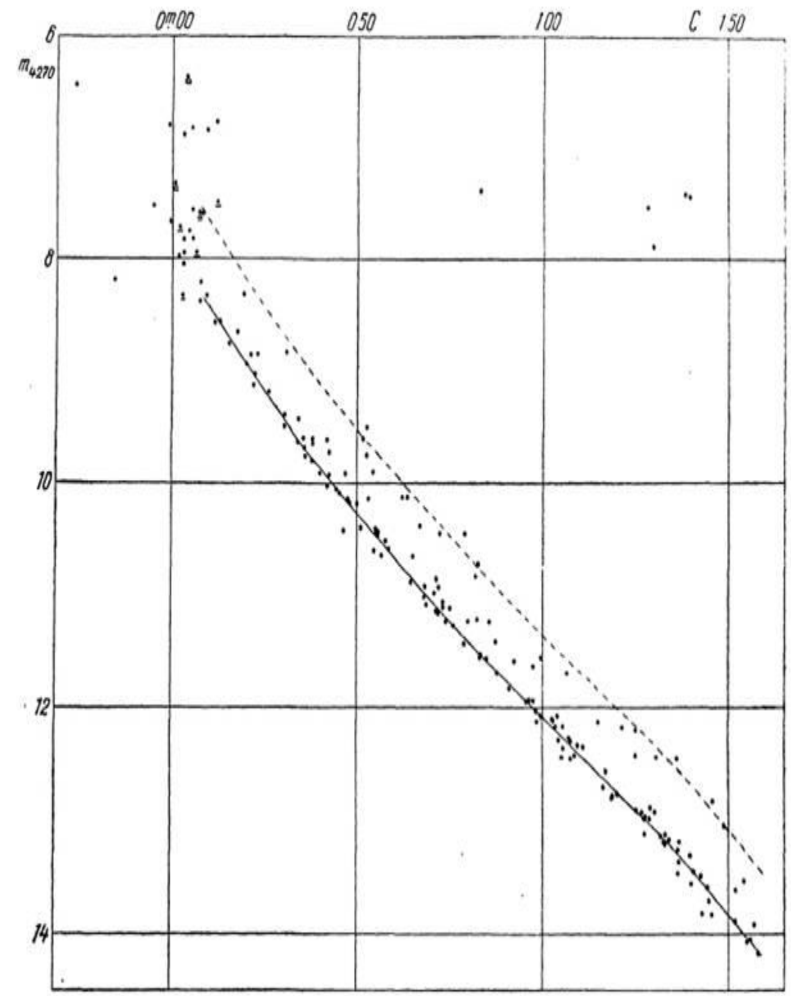

Observations of Praesepe with known binary systems

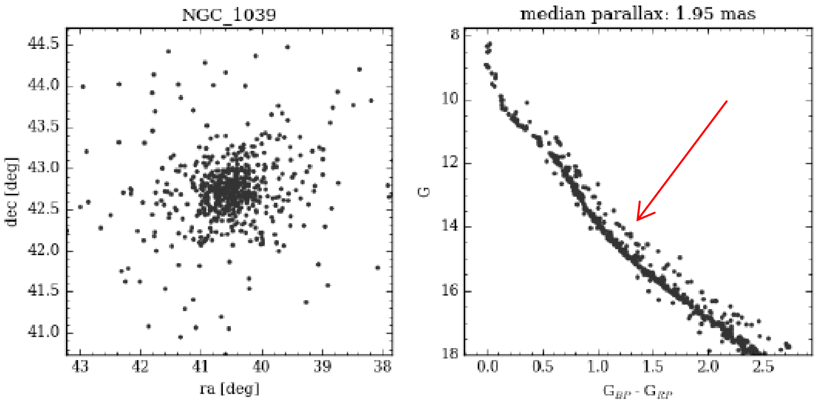

Fig. A.8. Left: distribution of the probable members of NGC 1039. Right: colour-magnitude diagram of the probable members.

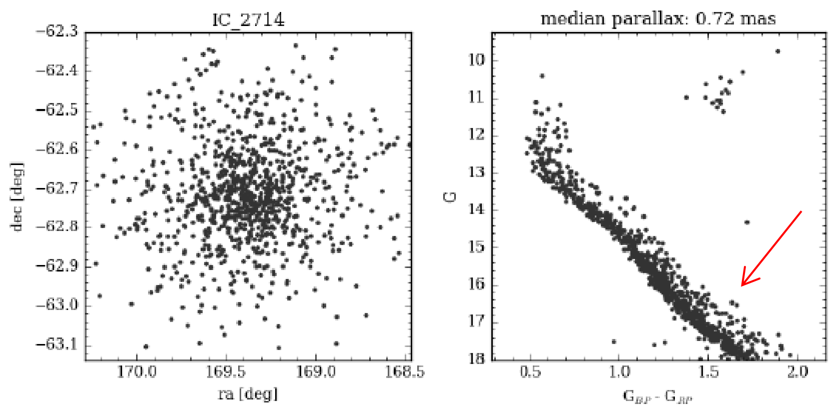

Fig. A.9. Left: distribution of the probable members of IC 2714. Right: colour-magnitude diagram of the probable members.

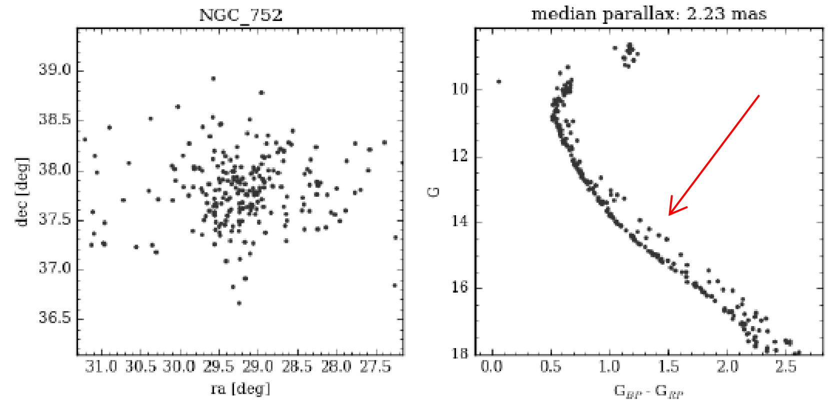

Fig. A.11. Left: distribution of the probable members of NGC 752. Right: colour-magnitude diagram of the probable members.

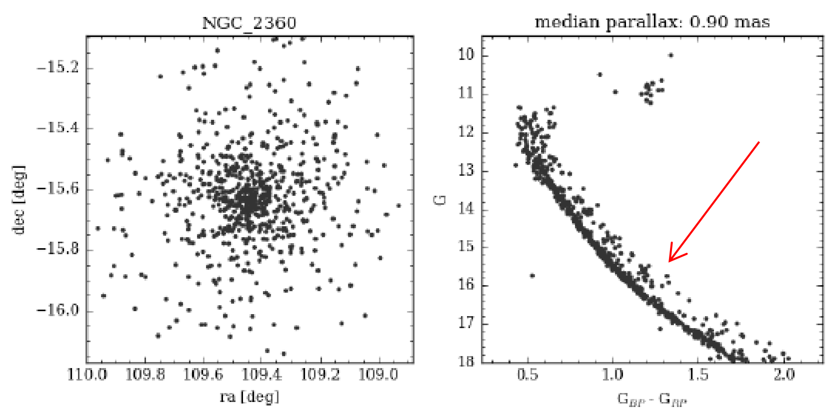

Fig. A.12. Left: distribution of the probable members of NGC 2360. Right: colour-magnitude diagram of the probable members.

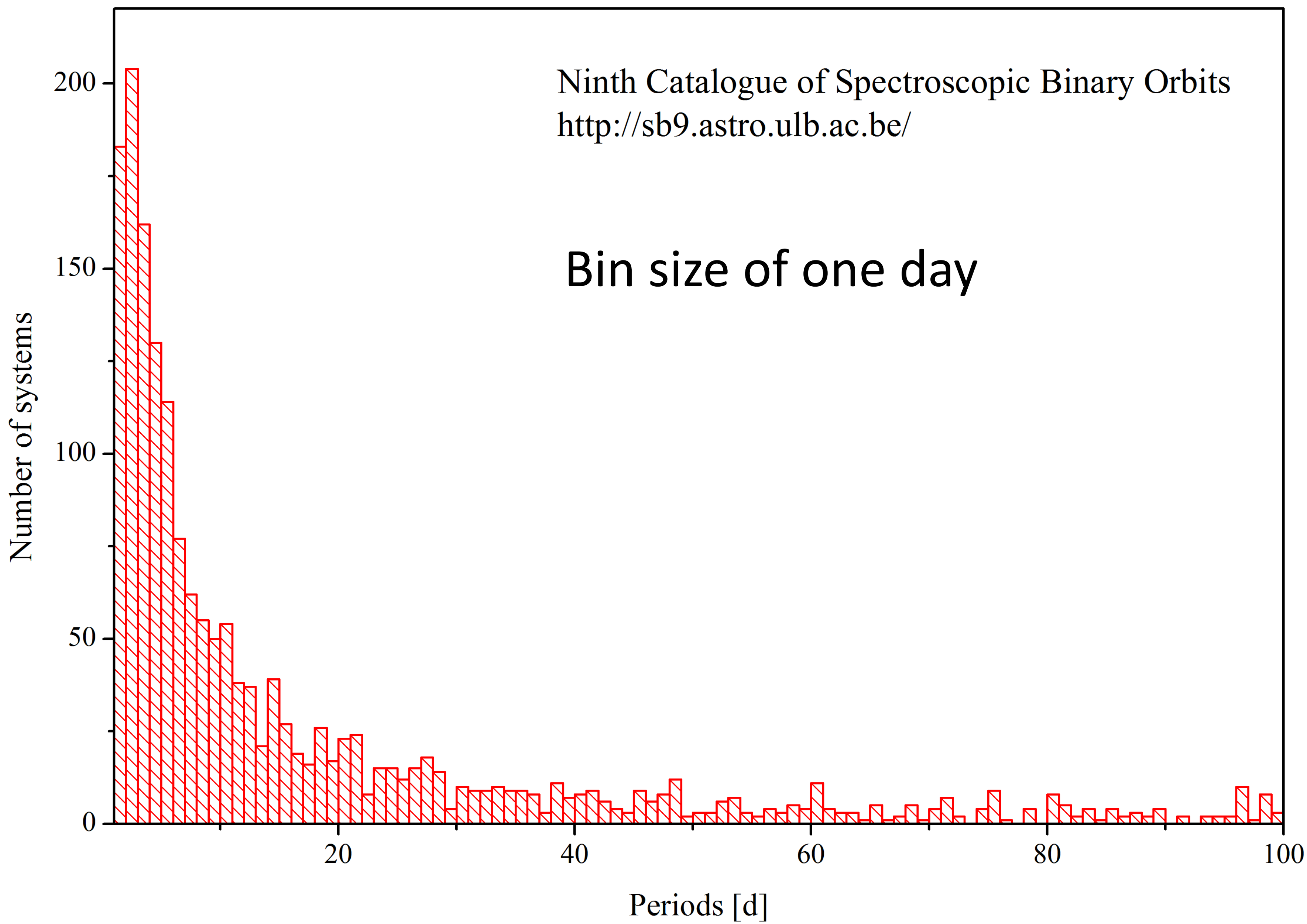
Ninth Catalogue of Spectroscopic Binary Orbits
http://sb9.astro.ulb.ac.be/
Bin size of one day
Number of systems
Periods [d]
0
50
100
150
200
20
40
60
80
100

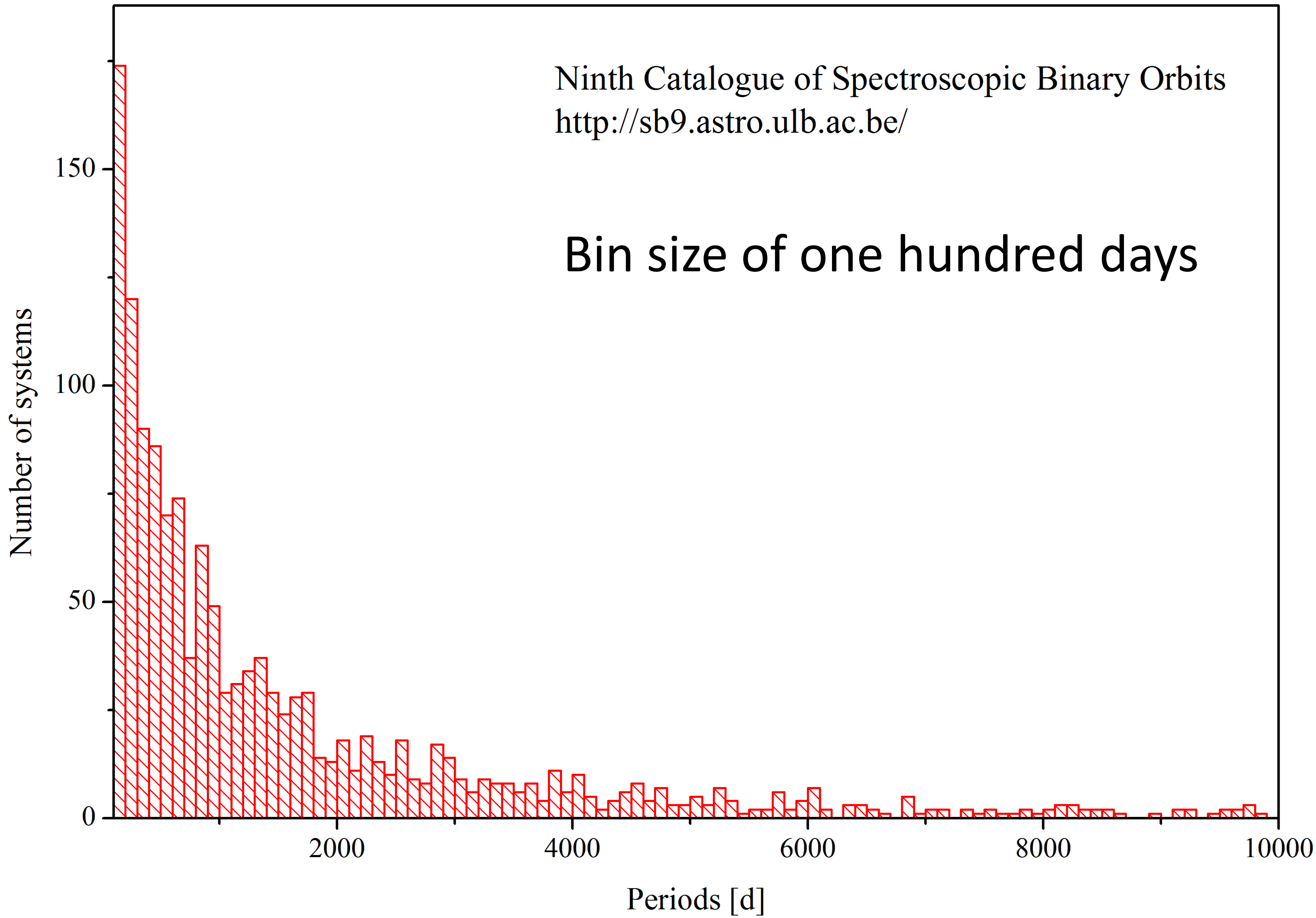

Ninth Catalogue of Spectroscopic Binary Orbits
http://sb9.astro.ulb.ac.be/
Bin size of one hundred days
Number of systems
0
50
100
150
2000
4000
6000
8000
10000
Periods [d]

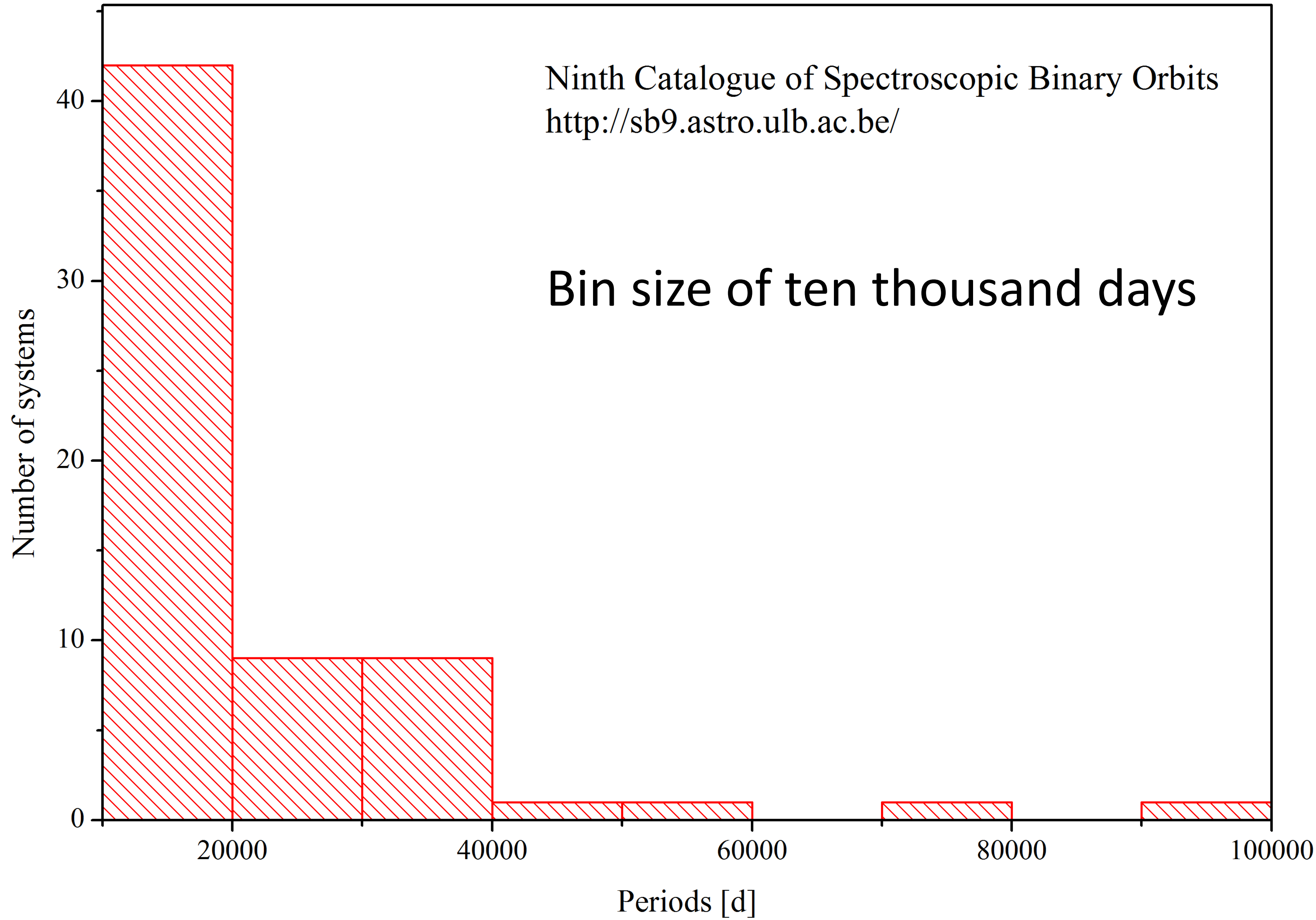
Ninth Catalogue of Spectroscopic Binary Orbits
http://sb9.astro.ulb.ac.be/
Bin size of ten thousand days
Number of systems
0
10
20
30
40
20000
40000
60000
80000
100000
Periods [d]

Results for open clusters

- Sollima et al., 2010, MNRAS, 401, 577
  - Cluster (log t): percentage
  - NGC 188 (9.63): 21 – 58%
  - NGC 2204 (9.20): 12 – 36%
  - NGC 2243 (9.58): 34 – 70%
  - NGC 2420 (9.08): 17 – 51%
  - NGC 2516 (8.52): 25 – 66%
- Sana et al., 2009, MNRAS, 400, 1479
  - NGC 6611 (6.50): 44 – 67%
- Sana et al., 2008, MNRAS, 386, 447
  - NGC 6231 (6.50): 63% - ?
- Bica & Bonatto, 2005, A&A, 431, 943
  - IC 4651 (9.26): 50 +- 11%
  - NGC 2287 (8.20): 48 +- 45%
  - NGC 2447 (8.60): 21 +- 9%
  - NGC 2548 (8.56): 48 +- 23%
  - NGC 2682 (9.51): 39 +- 16%
  - NGC 3680 (9.20): 25 +- 5%
  - NGC 5822 (9.00): 16 +- 8%
  - NGC 6208 (9.11): 54 +- 30%
  - NGC 6694 (7.85): 18 +- 12%
- Sandhu et al., 2003, A&A, 408, 515
  - NGC 2099 (8.60): ~30%
  - King 5 (9.00): ~30%
  - King 7 (8.80): ~20%

Globular clusters

r_h … Half-mass radius

f_b … binary fraction

Table 1
Fitting Results for Whole Field of View

Source	Size(in r_h)	$f_b\ (q > 0.5)$%	f_b (count)%	f_b (fit)%	Power x	$q_{\min}$	χ^2/dof	Note[a]
NGC 104	0.75	3.01 ± 0.13	8.04 ± 0.70	8.70 ± 0.50	−2.95 ± 0.05	0.28 ± 0.01	204.1/162	*d*
NGC 288	1.06	6.47 ± 0.31	12.87 ± 1.32	13.20 ± 0.60	−1.50 ± 0.09	0.27 ± 0.00	120.1/106	*g*
NGC 362	2.89	4.39 ± 0.16	8.28 ± 0.75	9.60 ± 0.30	−2.11 ± 0.19	0.24 ± 0.01	176.9/142	*d*
NGC 1851	4.64	2.88 ± 0.15	5.51 ± 0.82	6.50 ± 0.50	−2.91 ± 0.05	0.29 ± 0.01	126.4/136	*d*
NGC 2808	2.96	1.26 ± 0.18	−2.05 ± 0.66	0.50 ± 0.00	0.00 ± 3.00	0.77 ± 0.45	299.5/164	*d,p,e*
NGC 4590	1.57	8.12 ± 0.30	11.14 ± 1.27	13.30 ± 1.10	−2.48 ± 0.38	0.33 ± 0.00	141.6/96	*g*
NGC 5053	0.91	5.57 ± 0.40	8.09 ± 1.81	7.50 ± 1.50	−0.98 ± 0.75	0.33 ± 0.01	43.9/70	*g*
M3	1.02	5.10 ± 0.17	5.45 ± 0.70	6.80 ± 0.40	−2.11 ± 0.19	0.33 ± 0.00	200.3/161	*d*
NGC 5466	1.03	5.19 ± 0.35	8.96 ± 1.86	8.80 ± 1.60	−1.50 ± 0.38	0.30 ± 0.03	34.6/63	*g*
NGC 5897	1.15	5.74 ± 0.28	6.10 ± 1.27	7.10 ± 2.40	−0.75 ± 0.19	0.33 ± 0.01	100.4/98	*g*
NGC 5904	1.34	3.01 ± 0.14	4.61 ± 0.82	5.70 ± 1.20	−3.00 ± 0.05	0.30 ± 0.06	113.6/122	*d*
NGC 5927	2.15	2.44 ± 0.21	12.29 ± 0.93	14.20 ± 0.50	−3.00 ± 0.01	0.24 ± 0.01	157.3/148	*f*
NGC 6093	3.88	3.87 ± 0.18	1.42 ± 0.84	3.90 ± 0.30	−3.00 ± 0.09	0.40 ± 0.00	207.6/125	*d*
NGC 6121	0.55	4.78 ± 0.48	11.73 ± 2.16	16.20 ± 0.90	−3.00 ± 0.19	0.25 ± 0.01	66.0/62	*f*
NGC 6101	2.25	5.33 ± 0.23	6.54 ± 1.12	7.40 ± 0.40	−1.50 ± 0.19	0.31 ± 0.00	105.8/100	*g*
M13	1.40	3.28 ± 0.14	2.15 ± 0.71	2.50 ± 0.20	−2.81 ± 0.09	0.41 ± 0.01	147.1/145	*d*
NGC 6218	1.34	3.15 ± 0.22	8.51 ± 1.29	8.80 ± 0.90	−1.12 ± 0.38	0.18 ± 0.01	92.6/91	*g*
NGC 6341	2.32	4.12 ± 0.18	4.19 ± 0.69	4.40 ± 1.20	−1.03 ± 0.75	0.27 ± 0.03	247.0/146	*d*
NGC 6352	1.15	−0.58 ± 0.87	6.92 ± 2.09	5.50 ± 2.30	−1.88 ± 0.38	0.21 ± 0.06	110.4/99	*f*
NGC 6362	1.15	4.39 ± 0.29	11.21 ± 1.42	12.50 ± 1.70	−2.48 ± 0.09	0.24 ± 0.03	108.2/95	*g*
NGC 6397	0.82	4.48 ± 0.49	7.81 ± 1.81	10.90 ± 1.00	−3.00 ± 0.19	0.35 ± 0.00	103.1/79	*g*
NGC 6541	2.23	2.53 ± 0.19	5.57 ± 0.78	7.60 ± 0.30	−3.00 ± 0.02	0.27 ± 0.00	227.7/140	*d, f*
NGC 6624	2.89	1.57 ± 0.54	13.77 ± 1.32	27.30 ± 2.90	−2.98 ± 0.19	0.18 ± 0.03	200.2/144	*d, f*
NGC 6637	2.82	2.06 ± 0.30	5.53 ± 1.10	6.60 ± 0.40	−1.88 ± 0.19	0.18 ± 0.01	142.3/135	*d, f*
NGC 6652	4.93	0.87 ± 0.71	−0.03 ± 2.08	1.50 ± 0.50	0.00 ± 3.00	0.89 ± 0.45	92.7/85	*d, f*
NGC 6656	0.70	−4.87 ± 0.28	−0.69 ± 0.97	3.90 ± 1.40	−3.00 ± 0.05	0.18 ± 0.03	488.0/124	*f*
NGC 6723	1.55	4.55 ± 0.19	8.79 ± 0.97	10.20 ± 0.60	−3.00 ± 0.05	0.28 ± 0.00	113.2/118	*g*
NGC 6752	1.24	0.91 ± 0.16	2.97 ± 1.04	4.00 ± 0.50	−2.81 ± 0.19	0.25 ± 0.01	124.2/98	*g*
Terzan 7	3.07	12.23 ± 0.79	19.67 ± 2.62	19.10 ± 1.70	0.00 ± 0.19	0.18 ± 0.06	40.5/63	*g*
Arp 2	1.34	8.51 ± 0.55	8.32 ± 2.16	7.70 ± 1.60	0.00 ± 0.38	0.44 ± 0.23	57.9/74	*g*
NGC 6809	0.84	3.31 ± 0.22	3.10 ± 1.31	3.60 ± 0.30	0.00 ± 0.75	0.25 ± 0.06	64.8/77	*g*
NGC 6981	2.54	5.33 ± 0.24	5.50 ± 1.25	6.00 ± 0.40	−1.88 ± 0.75	0.38 ± 0.01	85.3/102	*d*
NGC 7078	2.37	4.38 ± 0.17	0.50 ± 0.62	1.50 ± 0.10	0.00 ± 0.19	0.25 ± 0.03	229.2/160	*d,e*
NGC 7099	2.30	3.06 ± 0.28	4.23 ± 1.08	5.20 ± 1.00	−3.00 ± 0.75	0.33 ± 0.06	85.7/68	*g*
Palomar12	1.38	13.44 ± 1.26	7.99 ± 4.25	15.90 ± 9.50	−0.75 ± 1.50	0.25 ± 0.45	13.1/33	*n*

Globular clusters

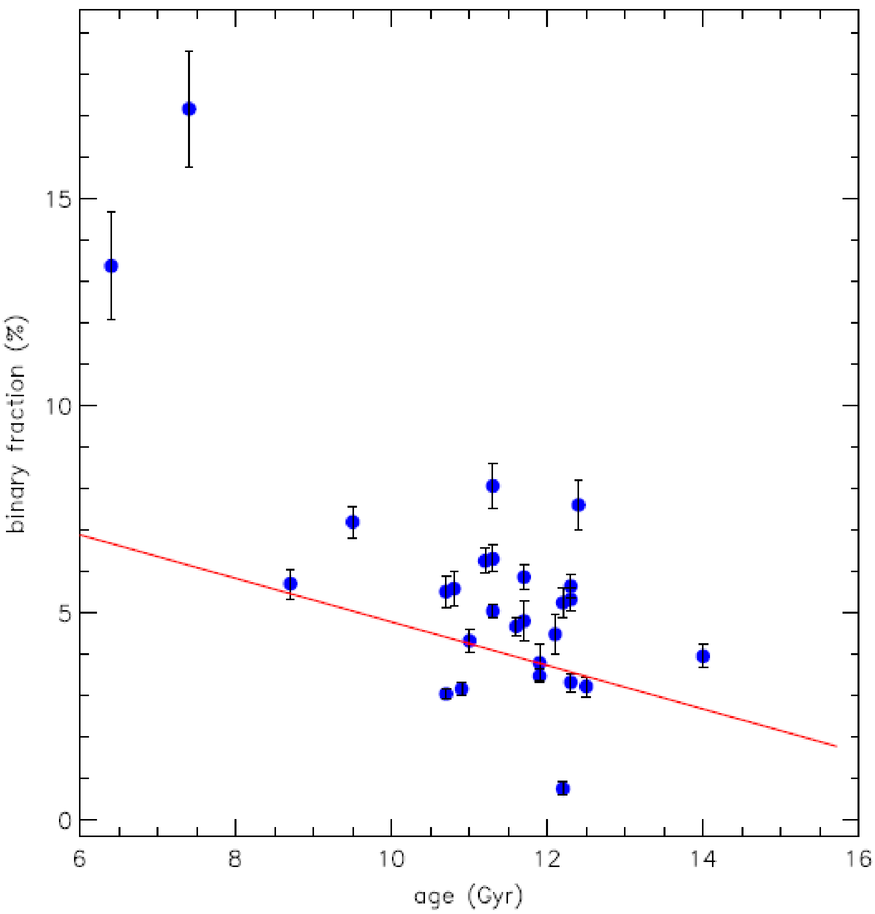

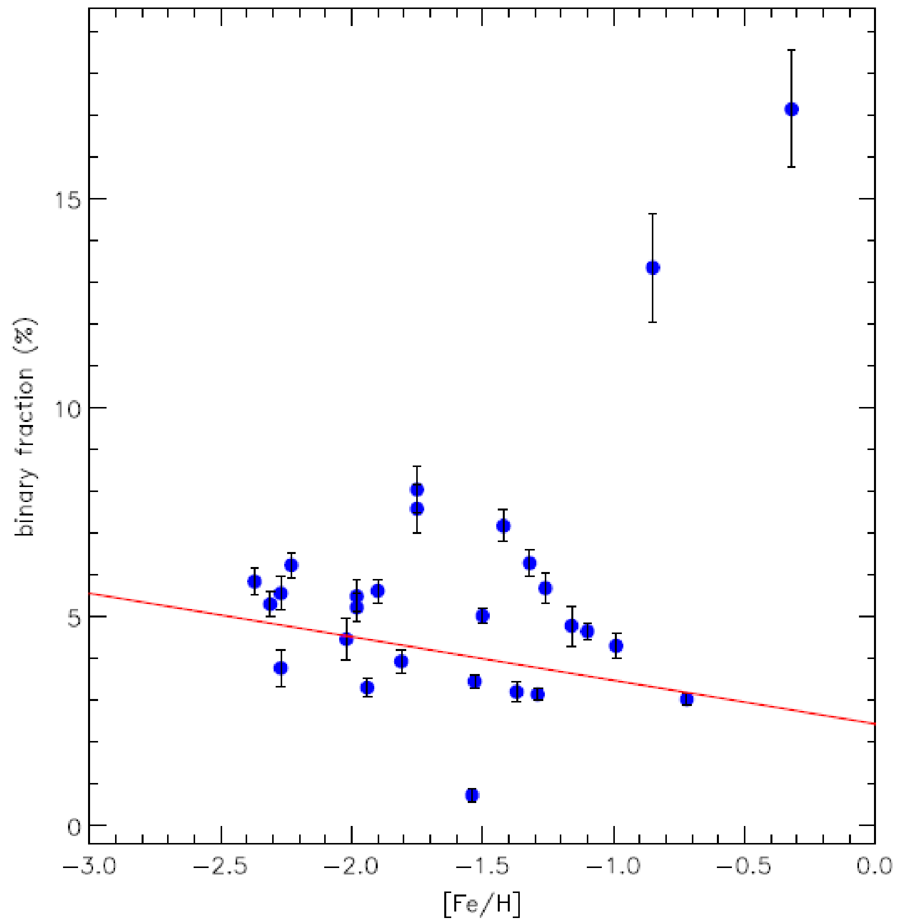

Globular clusters

r_h … Half-mass radius

f_b … binary fraction

Table 5
Fitting Results for Radial Bins

core ↓

Source	Bin Range (r_h)	f_b $(q > 0.5)$%	f_b (count)%	f_b (fit)%	χ^2/dof
NGC 104	0.00–0.29	4.14 ± 0.29	5.63 ± 1.27	4.19 ± 0.38	144.7/130
	0.29–0.42	2.72 ± 0.22	10.02 ± 1.25	11.94 ± 0.54	75.7/110
	0.42–0.56	2.11 ± 0.18	6.22 ± 1.26	10.59 ± 1.63	104.7/100
NGC 288	0.00–0.43	4.75 ± 0.51	4.51 ± 2.39	2.59 ± 0.98	64.0/63
	0.43–0.70	6.96 ± 0.58	17.21 ± 2.33	23.63 ± 2.32	77.0/71
	0.70–1.05	6.94 ± 0.55	18.69 ± 2.32	35.45 ± 8.90	38.8/67
NGC 362	0.00–0.97	5.74 ± 0.37	8.38 ± 1.34	6.53 ± 0.40	127.7/118
	0.97–1.48	4.57 ± 0.27	12.61 ± 1.32	15.76 ± 1.15	91.9/101
	1.48–2.16	2.53 ± 0.22	7.73 ± 1.33	10.37 ± 1.14	89.0/87
NGC 1851	0.00–1.55	3.80 ± 0.37	3.03 ± 1.47	2.84 ± 0.63	91.5/113
	1.55–2.34	2.20 ± 0.25	5.93 ± 1.45	8.62 ± 1.02	76.0/87
	2.34–3.55	1.50 ± 0.20	6.48 ± 1.45	8.74 ± 0.97	79.1/76
NGC 2808	0.00–1.35	−1.56 ± 0.38	−2.44 ± 1.19	0.50 ± 0.01	186.9/141
	1.35–1.73	1.14 ± 0.29	−1.08 ± 1.17	0.56 ± 0.14	180.3/132
	1.73–2.26	1.49 ± 0.28	−3.54 ± 1.17	0.50 ± 0.02	204.4/130
NGC 4590	0.00–0.44	8.27 ± 0.61	7.02 ± 2.30	5.42 ± 1.21	47.3/64
	0.44–0.74	3.88 ± 0.45	5.21 ± 2.30	6.90 ± 1.58	38.4/55
	0.74–1.14	6.40 ± 0.51	10.83 ± 2.28	19.70 ± 1.83	74.5/60
NGC 5053	0.00–0.36	5.64 ± 0.77	8.88 ± 3.24	5.91 ± 2.57	22.2/43
	0.36–0.52	4.71 ± 0.70	2.33 ± 3.31	6.41 ± 4.18	26.6/40
	0.52–0.68	4.90 ± 0.74	0.12 ± 3.32	5.42 ± 2.20	25.1/41
M3	0.00–0.35	6.17 ± 0.39	6.48 ± 1.26	5.44 ± 1.48	112.2/135
	0.35–0.54	3.94 ± 0.28	6.85 ± 1.25	9.21 ± 0.38	82.8/111
	0.54–0.76	3.62 ± 0.24	5.55 ± 1.25	8.37 ± 1.42	128.6/102
NGC 5466	0.00–0.39	5.09 ± 0.66	−0.48 ± 3.41	1.48 ± 1.48	31.8/39
	0.39–0.58	5.23 ± 0.66	3.02 ± 3.37	8.37 ± 4.37	24.6/38
	0.58–0.79	4.62 ± 0.62	1.96 ± 3.37	6.41 ± 4.51	34.4/39
NGC 5897	0.00–0.44	4.75 ± 0.56	2.11 ± 2.32	1.98 ± 0.67	41.0/63
	0.44–0.64	4.25 ± 0.49	5.92 ± 2.29	6.65 ± 0.98	29.6/59
	0.64–0.85	5.70 ± 0.51	7.40 ± 2.29	11.82 ± 1.72	32.6/61
NGC 5904	0.00–0.43	4.85 ± 0.35	1.94 ± 1.49	2.35 ± 1.47	75.4/103
	0.43–0.68	2.10 ± 0.24	6.11 ± 1.47	6.90 ± 1.40	75.9/78
	0.68–0.99	1.15 ± 0.18	4.09 ± 1.48	6.28 ± 2.12	52.3/67

Globular clusters

The Astrophysical Journal, 807:32 (13pp), 2015 July 1

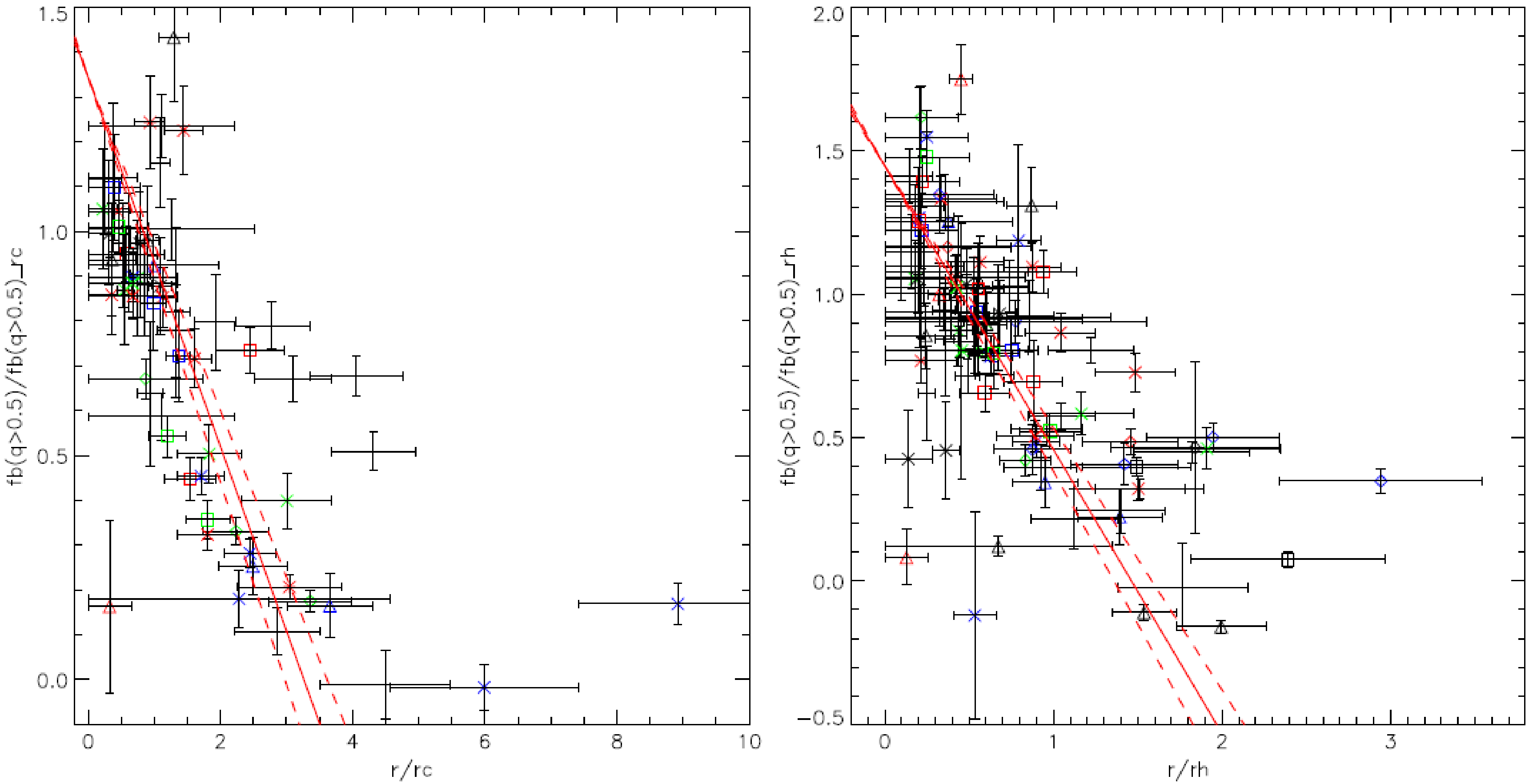

Figure 7. Combined high-mass-ratio ($q > 0.5$) binary fractions as a function of radius. Each cluster has three bins, with the same symbol and the same color on this figure. This strong relationship is similar to that found by Milone et al. (2012).